Annals of Glaciology 24 1997

Comparison of radio-echo sounding (30–1000 MHz) and high-resolution borehole-temperature measurements at Finsterwalderbreen, southern Spitsbergen, Svalbard

R. S. Ødegård,[1] J. O. Hagen,[2] S. -E. Hamran[3]
[1]*UNIS, P.O. Box 156, N-9170 Longyearbyen, Norway*
[2]*University of Oslo, Department of Geography, P.O. Box 1042, Blindern, N-0316 Oslo, Norway*
[3]*Environmental Surveillance Technology Programme, PFM, P.O. Box 89, N-2001 Lillestrøm, Norway*

ABSTRACT. Radio-echo soundings in four different frequency bands ranging from 30 to 1000 MHz were compared with temperature measurements in boreholes in the accumulation area and ablation area of Finsterwalderbreen (77°26′ N, 15°15′ E), southern Spitsbergen. Finsterwalderbreen is a polythermal surge-type glacier in the quiescent phase after its last surge around AD 1900. The objective of the study was to investigate the relation between internal echos and the glacier ice temperature to map the overall thermal structure of the glacier. The thermal structure is important for ice flow velocities and hydrology of glaciers, and it also affects their ability to surge. At the borehole site in the accumulation area (three boreholes within a range of 60 m), a change in the relative amplitude of the reflected signal is detected in the 320–370 and 600–650 MHz bands at 52–55 m depth. The high-resolution temperature measurements with 2 m intervals show that the transition zone between cold and temperate ice corresponds to the change in the relative amplitude on the 320–370 and 600–650 MHz bandwidth data. The overall thermal structure of the glacier was mapped based on the radar sounding. The radar results show (a) that the glacier is at the pressure-melting point over most of its bed except within 500–700 m of the terminus, and (b) that there is an upper cold ice layer of variable thickness (25–170 m) underlain by temperate ice. This thermal structure is confirmed by the thermistor-instrumented access holes to the bed in both the accumulation and ablation zones of the glacier. The variations in the thermal structure in lower parts of the accumulation area are explained by superimposed ice and ice layers that cause variations in the downward heat transfer by refreezing of meltwater.

INTRODUCTION

Water inclusions are known to have a strong influence on the absorption and scattering of radio waves, depending on frequency and bandwidth (Smith and Evans, 1972). An internal reflection horizon is common on Svalbard glaciers, and has been interpreted as being the boundary between surface cold ice and deeper ice containing liquid water (Dowdeswell and others 1984a, b; Bamber 1987a, b; Kotlyakov and Macheret 1987; Björnsson and others, 1996).

The thermal structure is important for ice flow velocities, hydrology and surging behaviour of glaciers. The main thermal characteristics of Svalbard glaciers are known, but there are still many unanswered questions with respect to the significance of the thermal regime, especially regarding the surge mechanism (Liestøl, 1969; Schytt, 1969; Hagen, 1987, 1988). Cold firn with minimal influence from percolating meltwater might exist locally on small ice caps at high altitude in Svalbard (1200–1600 m a.s.l.), but generally the large ice fields are known to be in the percolation or wet-snow zone in the altitude range 600–1200 m. a.s.l. (Sverdrup, 1935; Schytt, 1969; Liestøl, 1977, 1988; Hagen and Liestøl, 1990; Ødegård and others, 1992; Kameda and others, 1993; Björnsson and others, 1996). Previous measurements of glacier ice temperatures in the ablation zones show a cold surface layer (cf. Nixon and others, 1985). Deep boreholes in the ablation areas have documented a cold surface layer overlaying a temperate layer (Glazovskiy and Moskalevskiy, 1989; Björnsson and others, 1996). This confirms the early statement by Schytt (1969) on the polythermal nature of Svalbard glaciers, and the general description of the thermal regime given by Liestøl (1977). The cold surface layer extends into the lower parts of the accumulation area (Schytt, 1969; Ødegård and others, 1992) because the accumulation of superimposed ice or thick ice layers makes the firn impermeable to percolating meltwater, and hence there is no downward heat transfer by refreezing of meltwater. On small low-altitude glaciers like Austre Brøggerbreen near Ny-Ålesund, the winter cold wave is not eliminated even in the upper parts of the accumulation area (Björnsson and others, 1996), which cause net accumulation of cold ice.

The objective of the study was to investigate the relation between internal echoes and the glacier ice temperature to map the overall thermal structure of Finsterwalderbreen (Fig. 1), Svalbard. Three thermistor-instrumented access holes to the glacier bed were used to calibrate the radio-echo sounding (30–1000 MHz) relative to the thermal structure in both the accumulation and ablation zones of the glacier. Based on this calibration, the overall thermal structure of the glacier can be mapped from the radar soundings.

https://doi.org/10.3189/S0260305500012271 Published online by Cambridge University Press

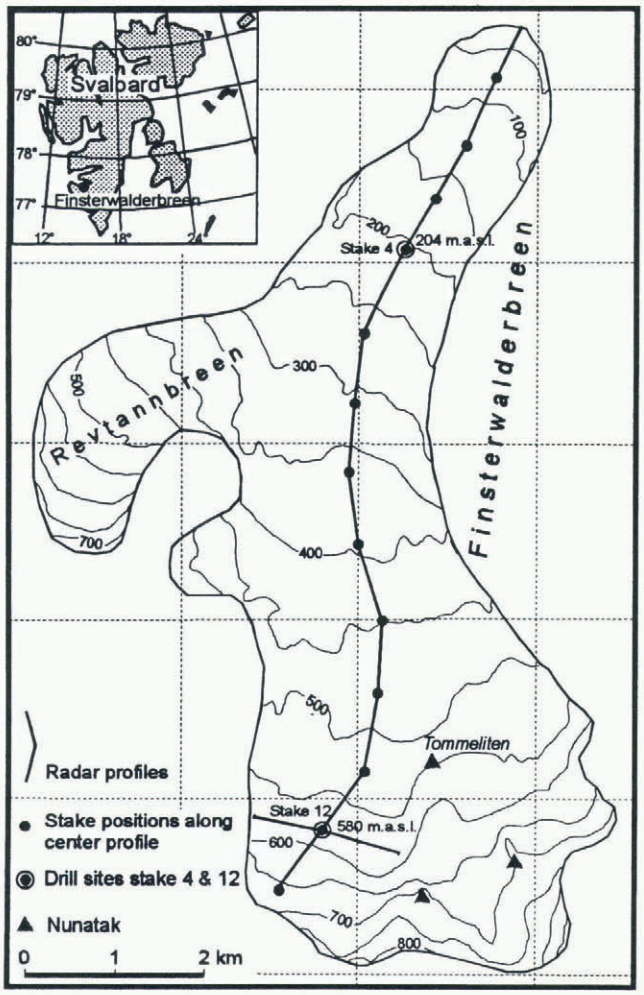

Fig. 1. Map of Finsterwalderbreen showing stake positions, radar profiles and drill sites.

DESCRIPTION OF FINSTERWALDERBREEN

Finsterwalderbreen (77°26′ N, 15°15′ E; Fig. 1) is an 11 km long, land-terminating glacier with an area of 35 km^2 which surged between 1898 and 1910 (Liestøl, 1969). The glacier is now in a quiescent phase (Hagen and others, 1993). The average ELA is 500 m a.s.l. (Nuttall and others, 1997). Mass-balance measurements were made by Norsk Polarinstitutt on Finsterwalderbreen every second year from 1950 to 1968, showing a total mass loss of 4.55 m w.e. during this period (results summarised in Hagen and Liestøl, 1990). Mean annual net mass balance from five ice cores in the accumulation area showed values of less than 0.25 m w.e. a^{-1} for the period 1962–63 to 1993 (Pinglot and others, 1997). These results indicate a negative mass balance in this century similar to that at Austre Brøggerbreen (Lefauconnier and Hagen, 1990).

RADAR SYSTEM

The radar system used is a time-gated synthetic pulse radar (Hamran 1989; Hamran and Aarholt, 1993; Hamran and others, 1995). The radar and antennae were mounted on a sledge pulled by a snowmobile. The horizontal distance between each measurement, controlled by a wheel on the sledge, was 4.2 m.

The frequency bandwidth of the system is 0.1 MHz–3 GHz. The antennae are the band-limiting factor for the sounding equipment. Three antennae are used to cover four frequency bands. An end-fed broad-bandwidth dipole is used from 30 to 80 MHz and a six-element yagi from 320 to 370 MHz. The two higher frequencies, 600–650 and 950–1000 MHz, are covered using a small log-periodic antenna having a bandwidth of 0.5–10 GHz. As the antenna gain-and-transfer function into the ice is not known for the antennae, absolute received power cannot be determined. Therefore, comparison of the amplitude between the different frequency bands is not possible, and only relative variations within the different frequency bands can be used. In the data reduction the dielectric constant of ice was assumed to be 3.2, giving a phase velocity of 168 $m\mu^{-1}s^{-1}$. The accuracy of estimated thickness of the cold surface layer is considered to be better than ± 4 m. The resolution of the measurements is 2 m. The zero reference altitude for the radio-echo sounding and the temperature measurements is the snow surface in late April 1994.

METHODS OF TEMPERATURE MEASUREMENT

Thermistor measurements were made in four access holes, two in the accumulation zone just 5 m apart (stake 12) and two in the ablation zone (stake 4 and at one site between stakes 1 and 2 at 108 m a.s.l.). This paper presents results from stakes 12 and 4 (Fig. 1). The results from the borehole between stakes 1 and 2 are not processed. The thermistor cable at stake 4 was installed on 23 April 1994 (198 m depth), and at stake 12 on 28 April 1994 and 2 April 1995 (100 and 52 m depth, 5 m apart).

Temperature measurements at stakes 12 (1994 borehole) and 4 were made with Fenwal Uni-curve thermistors with a resistance of 3.000 Ω at 25°C. The thermistors were individually calibrated at 5–6 points on the range from 0° to −20°C (including one calibration in an ice/water bath). The accuracy of the measurements is approximately ± 0.05°C. Temperature measurements at stake 12 (1995 borehole) were made with Fenwal Uni-curve thermistors with a resistance of 5.000 Ω at 25°C. The thermistors were precision-calibrated in the laboratory in a distilled-water/ice bath and the readings were made in a full bridge configuration using Campbell CR-10 data loggers. In the presentation a maximum error estimate of ± 0.03°C is used, including possible time-dependent drift in the fixed resistors, errors in the slope of the calibration curve and errors caused by the data loggers operating for short periods at ambient temperatures colder than the reference temperature of −25°C. Since measurements are made on the mV range they are subject to noise. Periods of noisy measurements are obtained on all channels, probably due to strain on the cable or vibration of the cable above the ice surface.

RESULTS

At stake 12 a change in the relative amplitude is detected at 52–55 m depth with the 320–370 and 600–650 MHz bandwidths, but a stronger signal is detected at greater depth (Fig. 2b and c). The radar-sounding results from the drill site at stake 12 (Fig. 2) were obtained by averaging the results within a range of 21 m from the borehole (42 m length, ten measurements). At 30–80 MHz frequencies a more diffuse increase in the relative amplitude is detected from 52 to 65 m depth (Fig. 2a). The results from the 950–1000 MHz bandwidth at stake 12 are noisy and difficult to interpret

https://doi.org/10.3189/S0260305500012271 Published online by Cambridge University Press

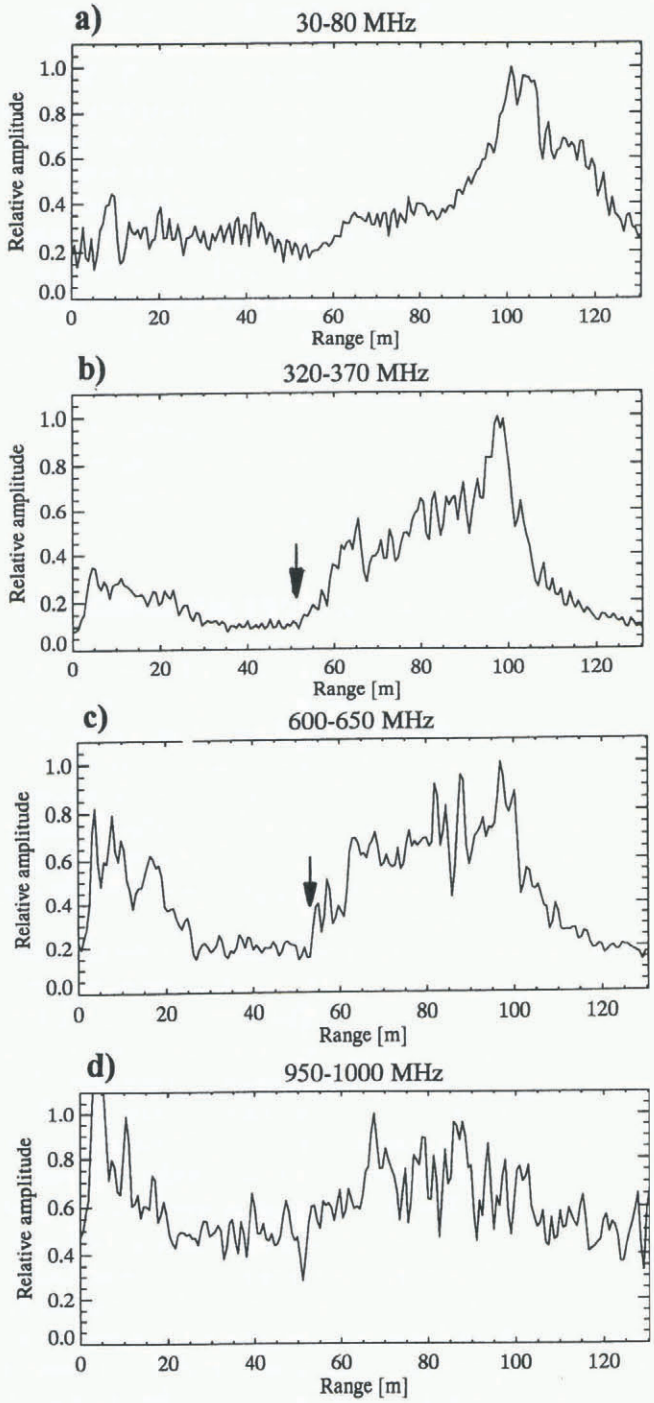

Fig. 2. Variations in relative radar amplitude at four different frequencies at the drill site at stake 12. The curves show the average of ten measurements within 21 m of the borehole.

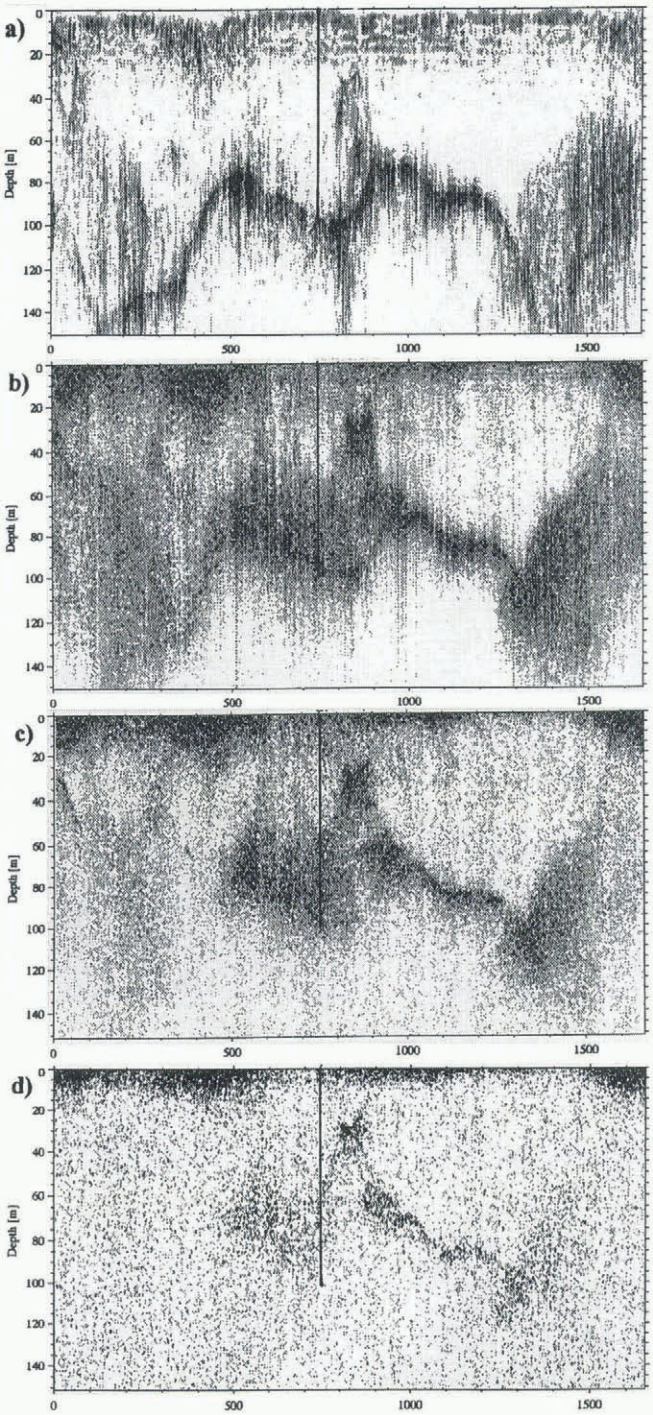

Fig. 3. Results of radar measurements at four different frequencies, (a) 30–80 MHz, (b) 320–370 MHz, (c) 600–650 MHz and (d) 950–1000 MHz, in a cross-profile at stake 12 (see Fig. 1). Vertical lines show drill site at stake 12 (100 m depth).

(Fig. 2d). The radar profiles are presented in Figures 3 and 4, showing the position of stake 12. At the cross-profiles the internal echo can be detected on all frequencies (Fig. 3a–d). It is not possible from these results to detect any frequency-dependent changes in the depth of the internal echo, but particularly on the 30–80 MHz data the internal echo is lost along most of the profile (Fig. 3a). The most distinct internal echoes are detected in the 320–370 and 600–650 MHz bands (Fig. 3b and c). Close to the margins of the glacier through the cross-profile at stake 12 the internal echo is missing except for a small zone of approximately 100 m at the eastern part of the profile (left part of Figure 3c). In the 950–1000 MHz band the internal echo can be detected along the central and eastern part of the profile (Fig. 3d).

The results of the temperature measurements at stakes 12 and 4 are shown in Figures 5 and 6. Both borehole sites have a two-layered thermal structure with a surface layer of cold ice underlain by a layer of ice at pressure-melting point (temperate ice). Based on the temperature measurements, the cold surface layer is 52–55 m thick at stake 12 in the accumulation area and 90–100 m thick at stake 4 in the ablation area (Figs 5 and 6). The internal echo is detected at corresponding depths (Figs 3 and 4). Exact extrapolation of the temperature measurements at stake 4 is difficult because there are no thermistors at 70–110 m depth.

An internal echo is detected along the whole profile ex-

https://doi.org/10.3189/S0260305500012271 Published online by Cambridge University Press

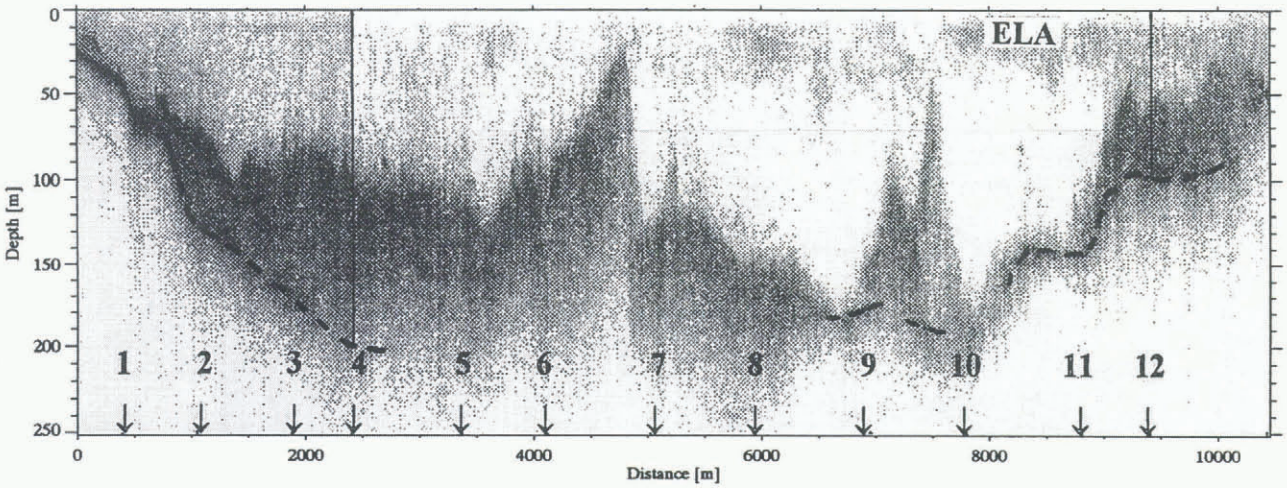

Fig. 4. Long profile of the glacier at 320–370 MHz, showing the internal echo and stake positions. Vertical lines show drill sites at stakes 4 (198 m depth) and 12 (100 m depth).

cept in a region near the front. In the ablation area, approximately 50% of the glacier ice is temperate along the centre flowline (Fig. 4). At a distance of 500–700 m from the front, the internal echo is difficult to distinguish from the bottom echo (left part of Figure 4). The internal echo is also difficult to distinguish from the bottom echo at two small spots near stakes 9 and 10 (Fig. 4). The depth of the internal echo ranges from 25 to 170 m. Large variations in the depth of the internal echo are detected both in the 1650 m long cross-profile at stake 12 and in the profile along the centre flowline. The largest gradient of the internal echo is detected between stakes 6 and 7, where the internal echo rises from 125 m depth to 25 m depth over a distance of 95–100 m.

INTERPRETATION AND DISCUSSION

Based on the high-resolution temperature measurements obtained from the borehole at stake 12 (Fig. 5) and the radar measurements at the same site (Figs 2–4), it has been shown that the internal echo represents the upper boundary of the temperate ice. At the borehole site an increase in relative amplitude of the 320–370 and 600–650 MHz measurements corresponds to the pressure-melting point isotherm within an error range of ± 2–4 m. Care should be taken, however, in the interpretation of the internal echo. The pressure-melting point isotherm corresponds to the *first* increase in relative amplitude (Fig. 2). Stronger signals are detected at greater depth at stake 12 (Fig. 2b and c). The interpretation of the internal echo as an indicator of the thermal structure of the glacier is in agreement with the interpretation of Holmlund and Eriksson (1989), Ødegård and others (1992) and Björnsson and others (1996) using the same or a similar radar. The depth to the glacier bed corresponds to the peak signal in relative amplitude at stake 12.

The results from the temperature and radar measurements at stake 12 show that an extensive cold surface layer can exist even at high altitude in the accumulation area of medium-size Svalbard glaciers. A large part of the accumulation area is dominated by the accumulation of superimposed ice, and there the surface meltwater does not percolate through the level of the winter cold wave. In Fig-

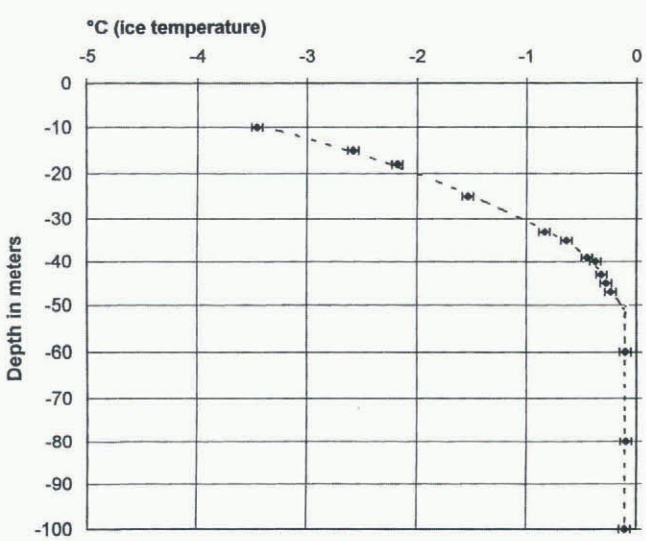

Fig. 5. Results of temperature measurements from two boreholes 5 m apart near stake 12 (see Fig. 1) in the accumulation area at 580 m a.s.l.

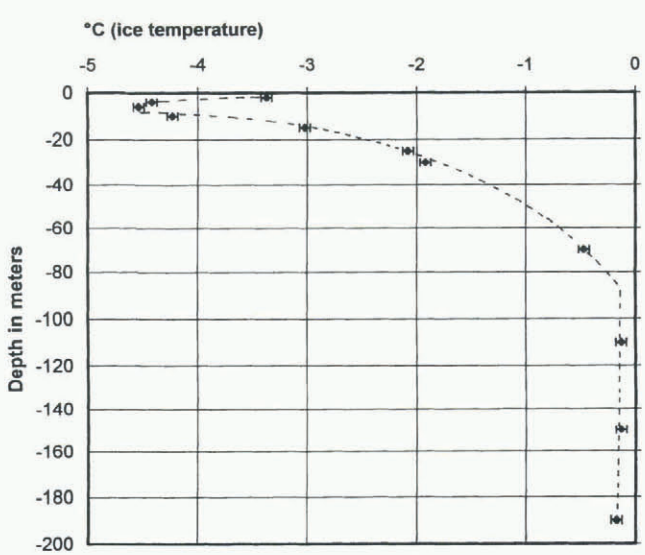

Fig. 6. Results of temperature measurements in the borehole at stake 4 in the ablation area 204 m a.s.l.

https://doi.org/10.3189/S0260305500012271 Published online by Cambridge University Press

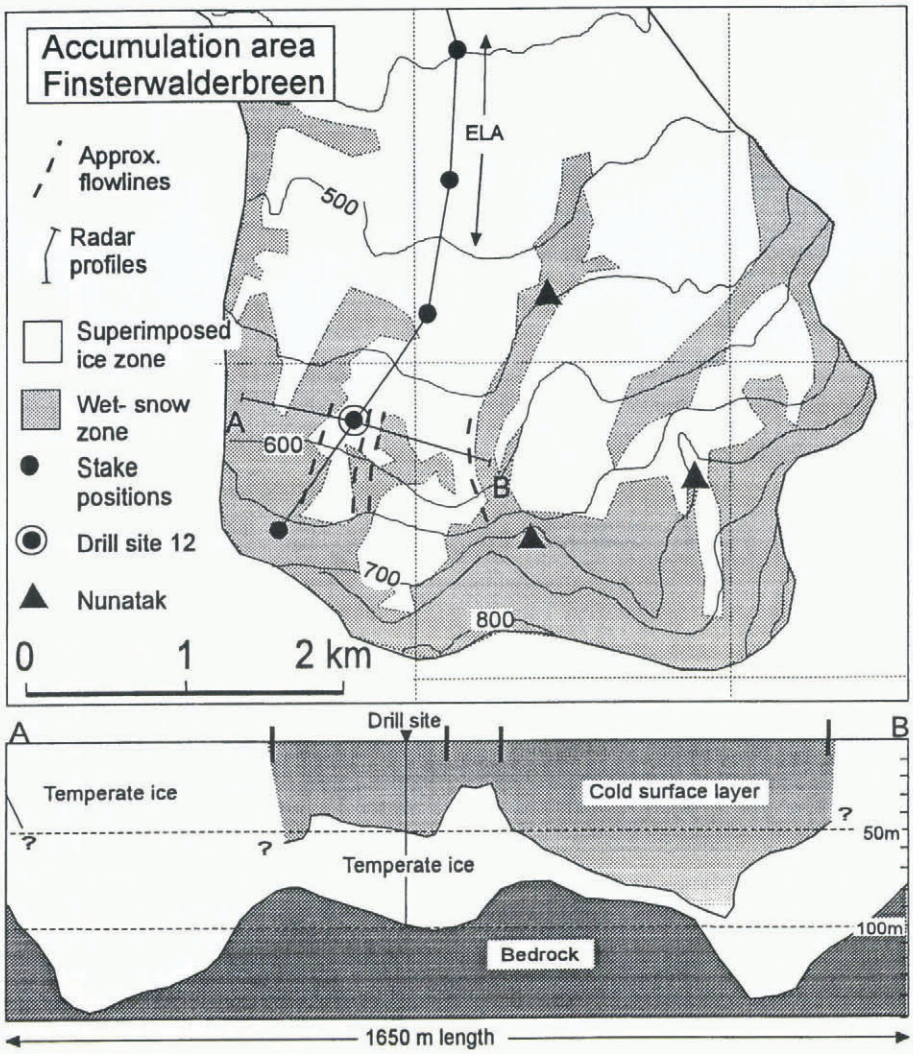

Fig. 7. Map of the accumulation area of Finsterwalderbreen and the interpretation of the cross-profile at stake 12. See text for discussion.

ure 7 the snowline is interpreted as an approximate border of the wet-snow zone. The snowline was taken from the Norsk Polarinstitutt map compiled from air photos taken in 1970 (Norsk Polarinstitutt, 1973). A similar distribution of the snowline is observed on air photos taken in autumn 1995.

The large lateral variations in the thermal structure of the glacier at the cross-profile at stake 12 (Figs 3 and 7) can be explained by the variations in the snowline. Different thermal characteristics can be identified depending on the altitude of the snowline (Fig. 7). The results show how sensitive the thermal structure is to local variations in the snow accumulation pattern. The marginal zones of the cross-profile appear to be composed of mostly temperate ice, because there is a large scatter in the radar measurements from the surface to approximately 20 m depth and no internal echo except over a distance of about 100 m at the western part. In these areas the snowline from the 1970 air photos is down-glacier from the profile. However, the internal echo could not be followed to the surface in the marginal zones, but disappears abruptly at 40–60 m depth. This problem of the interpretation was discussed by Björnsson and others (1996), and needs further attention. A very steep interface between cold and temperate ice is one possible interpretation.

At stake 12 the temperature gradient in the cold surface layer can be calculated from the measurements at 27 and 40 m depth to be $0.084^{\circ}\mathrm{C\,m^{-1}}$. A similar calculation in the ablation area shows a gradient of $0.034^{\circ}\mathrm{C\,m^{-1}}$ based on the measurements at 30 and 70 m depth at stake 4. A more accurate estimate of the temperature gradients at the base of the cold surface layer can be obtained from the thermistor cable at stake 12 installed in 1995, where the temperature gradient from the four lower thermistors range from 0.021° to $0.030^{\circ}\mathrm{C\,m^{-1}}$. Assuming a thermal conductivity of $2.1\,\mathrm{W\,K^{-1}\,m^{-1}}$, a latent heat of fusion of $3.0 \times 10^{8}\,\mathrm{J\,m^{-3}}$ and a 1–2% water content in the ice, the conductive heat transfer in the ice corresponds to a freezing rate of 0.2–0.6 m $\mathrm{a^{-1}}$ at the base of the cold surface layer. An accumulation rate of 0.2–0.3 m w.e. $\mathrm{a^{-1}}$ in the superimposed ice zone (Pinglot and others, 1997) gives a typical increase in the thickness of the cold surface layer within the range 0.4–0.9 m $\mathrm{a^{-1}}$ at stake 12. The lateral variations in the depth of cold surface layer in the cross-profile near stake 12 make it difficult to estimate an increase in the cold surface layer from the radio-echo sounding. However, the thickest cold surface layer is clearly detected in the lower parts of the accumulation area and in the upper parts of the ablation area (Fig. 4).

The temperature measurements at stake 4 in the ablation area show a cold surface layer of 90–100 m, which is in accordance with earlier measurements on surge-type glaciers in the Ny-Ålesund area. The calculated temperature gradient is $0.034^{\circ}\mathrm{C\,m^{-1}}$ at 30–70 m depth, which gives

https://doi.org/10.3189/S0260305500012271 Published online by Cambridge University Press

a small upward heat flux of less than 0.1 W m^{-2} at the base of the cold surface layer. This calculation indicates that the freezing of the temperate ice at the base of the cold surface layer is not in equilibrium with the surface melt in the ablation area. The emergence velocity in the lower ablation area is more than 1 m a^{-1}. A thinning of the cold surface layer is detected towards the front of the glacier (Fig. 4). The extent of the temperate ice layer relative to the cold surface layer of Finsterwalderbreen suggests that the polythermal nature of the glacier does not have a strong influence on the deformation velocities in the ablation area. The cold surface layer is probably of more significance to the hydrology by reducing the amount of water reaching the glacier and influencing the spatial distribution of water reaching the glacier bed. This coupling to the hydrological system could be highly significant to the surge mechanism and needs further attention.

CONCLUSIONS

Comparison of radio-echo sounding (30–1000 MHz) and high-resolution borehole-temperature measurements at a drill site in lower parts of the accumulation area shows that the *first* change in the relative amplitude detected in the 320–370 and 600–650 MHz signals corresponds to the pressure-melting point isotherm at 52–55 m depth within an error range of ±2–4 m. A stronger signal is detected at greater depth, particularly at the 320–370 MHz signals.

The overall thermal structure of the glacier was mapped based on an interpretation of the internal echo as the top of the temperate ice layer. The radar results show (a) that the glacier is at the pressure-melting point over most of its bed except within 500–700 m of the terminus and (b) that there is an upper cold ice layer of variable thickness underlain by temperate ice. The thickness of the cold surface layer ranges from 25 to 170 m. In a 1650 m long cross-profile in the accumulation area, entirely temperate ice and ice with a cold surface layer with a maximum thickness of more than 90 m are found (Figs 3 and 7). Variations in the thermal structure in the lower parts of the accumulation area are mainly explained by superimposed ice and ice layers that cause variations in the downward heat transfer by refreezing of meltwater. Superimposed ice and ice layers are mainly controlled by local variations in snow accumulation.

Based on the temperature measurements, the freezing rate at the base of the cold surface layer could be estimated to be more than 0.2 m a^{-1} at stake 12. When the net surface mass balance is taken into account this shows the general pattern of increasing thickness of the cold layer in the lower accumulation area and upper ablation area, while a thinning occurs in the lower ablation area of the glacier. This is confirmed by the radio-echo soundings, showing thickest cold ice layers in the lower accumulation area and upper ablation area, and a gradual thinning downstream.

ACKNOWLEDGEMENTS

This study was conducted as part of the European Union Environment Programme under the project "Investigations of Glacier Surges: Measurements and Modelling of Ice Dynamics in Svalbard, European Arctic", grant EN5V-CT93-0299. The radar was developed by the Royal Norwegian Council for Scientific and Industrial Research, Environmental Surveillance Technology Program. We thank A. -M. Nuttall and J. L. Wadham for assistance in the field and A. -M. Nuttall for help with the English manuscript.

REFERENCES

Bamber, J. L. 1987a. Internal reflecting horizons in Spitsbergen glaciers. *Ann. Glaciol.*, **9**, 5–10.

Bamber, J. L. 1987b. Radio echo sounding studies of Svalbard glaciers. (Ph.D. thesis, University of Cambridge.)

Björnsson, H. *and 6 others*. 1996. The thermal regime of sub-polar glaciers mapped by multi-frequency radio-echo sounding. *J. Glaciol.*, **42**(140), 23–32.

Dowdeswell, J. A., D. J. Drewry, O. Liestøl and O. Orheim. 1984a. Airborne radio echo sounding of sub-polar glaciers in Spitsbergen. *Nor. Polarinst. Skr.* 182.

Dowdeswell, J. A., D. J. Drewry, O. Liestøl and O. Orheim. 1984b. Radio echo-sounding of Spitsbergen glaciers: problems in the interpretation of layer and bottom returns. *J. Glaciol.*, **30**(104), 16–21.

Glazovskiy, A. F. and M.Yu. Moskalevskiy. 1989. Issledovaniya lednika Frit'of na Shpitsbergene v 1988 godu [Studies of Fridtjovbreen on Spitsbergen in 1988]. *Mater. Glyatsiol. Issled.* 65, 148–153.

Hagen, J. O. 1987. Glacier surge at Usherbreen, Svalbard. *Polar Res.*, **5**(2), 239–252.

Hagen, J. O. 1988. Glacier surge in Svalbard with examples from Usherbreen. *Nor. Geogr. Tidsskr.*, **42**(4), 203–213.

Hagen, J. O. and O. Liestøl. 1990. Long-term glacier mass-balance investigations in Svalbard, 1950–88. *Ann. Glaciol.*, **14**, 102–106.

Hagen, J. O., O. Liestøl, E. Roland and T. Jørgensen. 1993. Glacier atlas of Svalbard and Jan Mayen. *Nor. Polarinst. Medd.* 129.

Hamran, S.-E. 1989. Geophysical electromagnetic backscatter tomography: experimental results from glacier study. (D.Sc. thesis, University of Tromsø.)

Hamran, S.-E. and E. Aarholt. 1993. Glacier study using wavenumber domain synthetic aperture radar. *Radio Sci.*, **28**(4), 559–570.

Hamran, S.-E., D. T. Gjessing, J. Hjelmstad and E. Aarholt. 1995. Ground penetrating synthetic pulse radar: dynamic range and modes of operation. *J. Appl. Geophys.*, **33**, 7–14.

Holmlund, P. and M. Eriksson. 1989. The cold surface layer on Storglaciären. *Geogr. Ann.*, **71A**(3–4), 241–244.

Kameda, T., S. Takahashi, K. Goto-Azuma, S. Kohshima, O. Watanabe and J. O. Hagen. 1993. First report of ice core analyses and borehole temperatures on the highest icefield on western Spitsbergen in 1992. *Bull. Glacier Res.* 11, 51–61.

Kotlyakov, V. M. and Yu.Ya. Macheret. 1987. Radio echo-sounding of subpolar glaciers in Svalbard: some problems and results of Soviet studies. *Ann. Glaciol.*, **9**, 151–159.

Lefauconnier, B. and J. O. Hagen. 1990. Glaciers and climate in Svalbard: statistical analysis and reconstruction of the Brøggerbreen mass balance for the last 77 years. *Ann. Glaciol.*, **14**, 148–152.

Liestøl, O. 1969. Glacier surges in west Spitsbergen. *Can. J. Earth Sci.*, **6**(4), Part 2, 895–897.

Liestøl, O. 1977. Pingos, springs and permafrost in Spitsbergen. *Nor. Polarinst. Årbok* 1975, 7–29.

Liestøl, O. 1988. The glaciers in the Kongsfjorden area, Spitsbergen. *Nor. Geogr. Tidsskr.*, **42**(4), 231–238.

Nixon, W. A. *and 6 others*. 1985. Applications and limitations of finite element modeling to glaciers: a case study. *J. Geophys. Res.*, **90**(B13), 11,303–11,311.

Norsk Polarinstitutt. 1973. *Finsterwalderbreen*. Oslo, Norsk Polarinstitutt. (Map sheet, Scale 1:10 000.)

Nuttall, A.-M., J. O. Hagen and J. A. Dowdeswell. 1997. Quiescent-phase changes in velocity and geometry of Finsterwalderbreen, a surge-type glacier in Svalbard. *Ann. Glaciol.*, **24**, (see paper in this volume).

Ødegård, R. S., S.-E. Hamran, P. H. Bø, B. Etzelmüller, G. Vatne and J. L. Sollid. 1992. Thermal regime of a valley glacier, Erikbreen, northern Spitsbergen. *Polar Res.*, **11**(2), 69–79.

Pinglot, J. F., M. Pourchet, B. Lefauconnier and M. Creseveur. 1997. Equilibrium line and mean annual mass balance of Finsterwalderbreen, Spitsbergen, determined by in situ and laboratory gamma-ray measurements of nuclear test deposits. *Ann. Glaciol.*, **24** (see paper in this volume).

Schytt, V. 1969. Some comments on glacier surges in eastern Svalbard. *Can. J. Earth Sci.*, **6**(4), Part 2, 867–873.

Smith, B.M.E. and S. Evans. 1972. Radio echo sounding: absorption and scattering by water inclusion and ice lenses. *J. Glaciol.*, **11**(61), 133–146.

Sverdrup, H. U. 1935. Scientific results of the Norwegian–Swedish Spitsbergen Expedition in 1934. Part III. The temperature of the firn on Isachsen's Plateau, and general conclusions regarding the temperature of the glaciers on West-Spitzbergen. *Geogr. Ann.*, **17**(1–2), 53–88.

https://doi.org/10.3189/S0260305500012271 Published online by Cambridge University Press